ONLINE SUPPLEMENTARY MATERIAL

EXPLOITING ANTIGENIC DIVERSITY FOR VACCINE DESIGN: THE CHLAMYDIA ARTJ PARADIGM

Marco Soriani, Pierre Petit[1], Renata Grifantini[†], Roberto Petracca, Giovanni Gancitano, Elisabetta Frigimelica, Filomena Nardelli, Christel Garcia[1], Silvia Spinelli[2], Guido Scarabelli[3], Sebastien Fiorucci[4‡], Roman Affentranger[5], Mario Ferrer-Navarro[5], Martin Zacharias[4°], Giorgio Colombo[3], Laurent Vuillard[1], Xavier Daura [5,6] and Guido Grandi

Novartis Vaccines, Via Fiorentina 1, 53100, Siena, Italy; [1]BioXtal Structural Biology unit. c/o AFMB, UMR 6098, CNRS-Universités Aix-Marseille I & II, Campus de Luminy, 13288 Marseille Cedex 09, France; [2]AFMB, UMR 6098, CNRS-Universités Aix-Marseille I & II, Campus de Luminy, 13288 Marseille Cedex 09, France; [3]Istituto di Chimica del Riconoscimento Molecolare, CNR. Via Mario Bianco 9, 20131 Milano, Italy; [4]Jacobs University Bremen, Campus Ring 6, D-28759 Bremen, Germany ; [5]Institute of Biotechnology and Biomedicine (IBB), Universitat Autònoma de Barcelona (UAB), 08193 Bellaterra, Spain; [6]Catalan Institution for Research and Advanced Studies (ICREA), 08010 Barcelona, Spain

[†] Current address: Externautics Spa, Via Fiorentina 1, 53100, Siena, Italy

[‡] Current address: LCMBA, UMR 6001, Université de Nice Sophia Antipolis, 06108 Nice Cedex 2, France

[°] Current address: Technische Universität München, 85748 Garching, Germany

Running head: A new structure-based approach for vaccine design

Address correspondence to: Guido Grandi, Novartis Vaccines and Diagnostics, Via Fiorentina 1, 53100, Siena, Italy. Tel: +390577243390. Fax: +390577243564. E-mail: guido.grandi@novartis.com

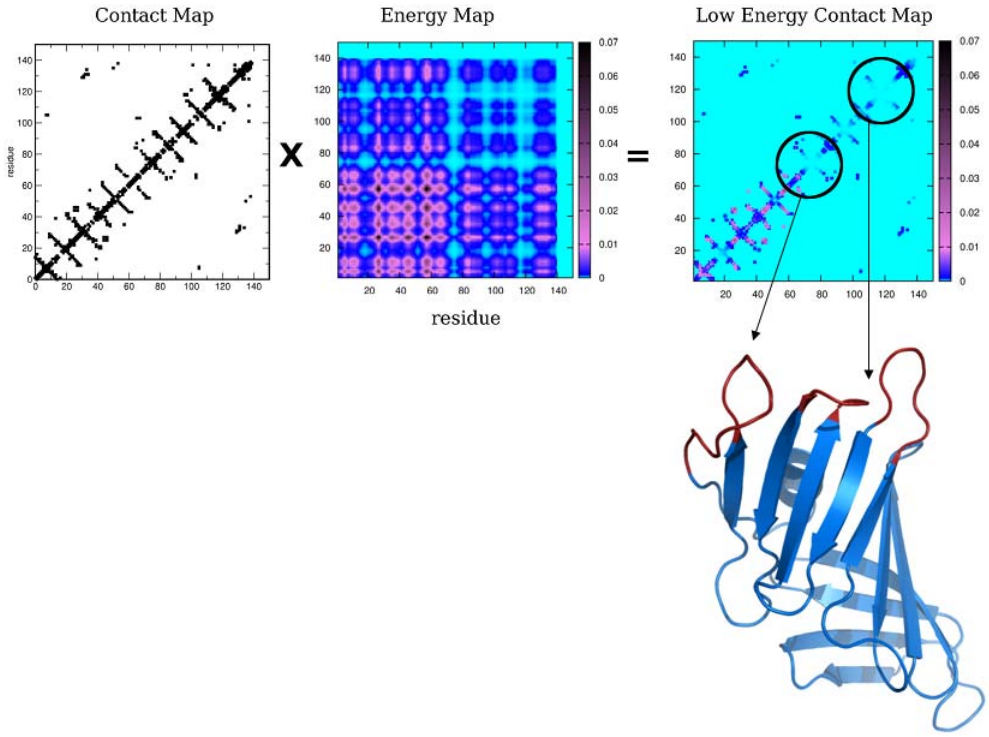

Figure S1. Schematic representation of the energy-decomposition-based epitope-prediction method. The contact map is multiplied by the simplified energy-coupling matrix. The resulting matrix reports the energetic coupling intensity of two residues in contact in space, represented as a colour scale assigned to each point of the matrix. The weakest local interactions vanish in the background colour: predicted epitopes are identified with circles. The arrows indicate the projections of the predicted epitope regions on the 3D structure of the protein.

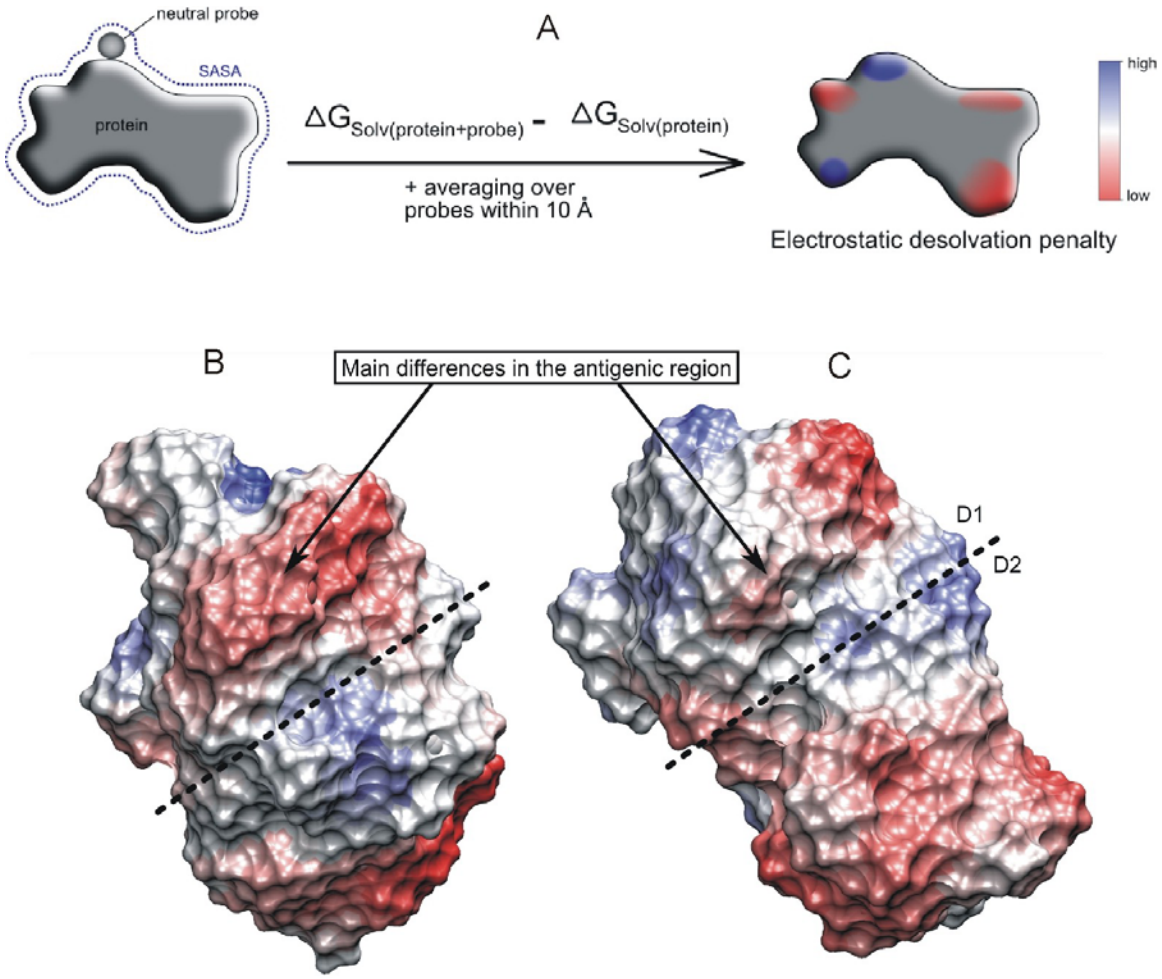

Figure S2: (A) Schematic illustration of the electrostatic desolvation caculation of a neutral probe placed at the protein surface. Regions with low electrostatic desolvation free energy appear in red while those with high penalty are blue. Desolvation surface profiles of CPn ArtJ (B) and CT ArtJ (C). The calculated profiles of both proteins exhibit some differences in the D1 domain, suggesting a larger desolvation penalty of CT ArtJ compared to CPn ArtJ. The dashed line marks the boundary between domains D1 and D2.

A

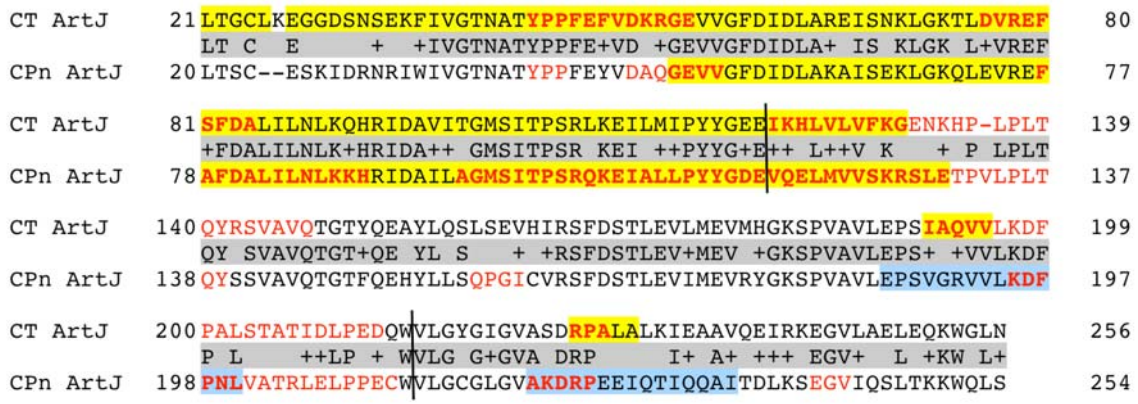

B

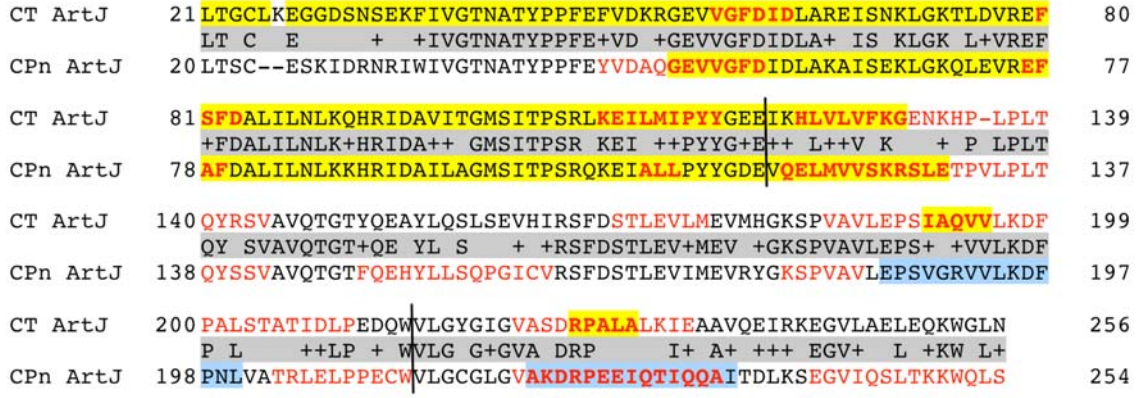

Figure S3. Graphical representation of the experimental and computational epitope mappings of CT and Cpn ArtJ. Sequence alignment of the two proteins with conserved residues in middle row. The beginning and end of D2 are marked with vertical lines. Experimentally determined epitopes are identified by a yellow background in both (A) and (B). Very low reactivity regions of CPn ArtJ are colored in light blue. (A) Epitope regions predicted by the energy-decomposition method are shown in red font, and highlighted bold when they overlap with experimentally determined epitope regions. (B) Epitope regions predicted by the electrostatic-desolvation free-energy method are shown in red font, and highlighted bold when they overlap with experimentally determined epitope regions.

Table S1. Computational epitope mapping.

Energy-decomposition-based prediction	
CT ArtJ regions	**CPn ArtJ regions**
44-YPPFEFVDKRGE-55	41-YPP-43
76-DVREFSFDA-84	48-DAQGEVV-54
121-IKHLVLVFKGENKHPLPLTQYRSVAVQ-147	77-FAFDALILNLKKH-89
191-IAQVVLKDFPALSTATIDLPED-212	96-AGMSITPSRQKEIALLPYYGDEVQELMVVSKR
226-RPA-228	SLETPVLPLTQY-139
	157-QPGI-160
	195-KDFPNLVATRLELPPEC-211
	221-AKDRP-225
	241-EGV-243
Electrostatic-desolvation-based prediction	
CT ArtJ regions	**CPn ArtJ regions**
57-VGFDID-62*	46-YVDAQGEVVGFD-57*
80-FSFD-83*	76-EFAF-79*
109-KEILMIPYYGE-119	109-ALL-111
123-HLVLVFKGENKHLPLTQYRSV-144	119-QELMVVSKRSLETPVLPLTQYSSV-142
169-STLEVLM-175	149-FQEHYLLSQPGICV-162
184-VAVLEPSIAQVVLKDFPALSTATIDLP-210	179-KSPVAV-184
222-VASDRPALALKIE-234	203-TRLELPPECW-212
	220-VAKDRPEEIQTIQQA-234
	241-EGVIQSLTKKWQLS-254*

*Predicted for isolated domains

Table S2. Characterization of the epitopes predicted by the two computational methods.

	Energy-decomposition-based perdiction		Desolvation-penalty-based prediction	
	CT ArtJ	CPn ArtJ	CT ArtJ	CPn ArtJ
Epitopes in D1	3	6	4	5
Epitopes in D2	2	3	3	4
Epitopes in D1 overlapping experimental ones	3	4	4	4
Epitopes in D2 overlapping experimental ones	2	2	2	1
Residues in D1 epitopes	24	53	34	48
Residues in D2 epitopes	49	43	53	54
Residues in D1 epitopes overlapping experimental ones	24	44	26	28
Residues in D2 epitopes overlapping experimental ones	15	19	13	10
Epitopes in D1 not overlapping with those in the ortholog protein	0	2	0	1
Epitopes in D2 not overlapping with those in the ortholog protein	0	1	1	1
Epitope residues in D1 not overlapping with those in the ortholog protein	9	38	11	25
Epitope residues in D2 not overlapping with those in the ortholog protein	12	7	25	22